ARMY RESEARCH LABORATORY

Beacon Position and Attitude Navigation Aided by a Magnetometer

by Xu Ma and Gonzalo R. Arce

ARL-CR-650 **June 2010**

NOTICES

Disclaimers

The findings in this report are not to be construed as an official Department of the Army position unless so designated by other authorized documents.

Citation of manufacturer's or trade names does not constitute an official endorsement or approval of the use thereof.

Destroy this report when it is no longer needed. Do not return it to the originator.

Army Research Laboratory

Aberdeen Proving Ground, MD 21005-5066

ARL-CR-650   **June 2010**

Beacon Position and Attitude Navigation Aided by a Magnetometer

Xu Ma and Gonzalo R. Arce
University of Delaware

prepared by

REPORT DOCUMENTATION PAGE			*Form Approved* *OMB No. 0704-0188*
Public reporting burden for this collection of information is estimated to average 1 hour per response, including the time for reviewing instructions, searching existing data sources, gathering and maintaining the data needed, and completing and reviewing the collection information. Send comments regarding this burden estimate or any other aspect of this collection of information, including suggestions for reducing the burden, to Department of Defense, Washington Headquarters Services, Directorate for Information Operations and Reports (0704-0188), 1215 Jefferson Davis Highway, Suite 1204, Arlington, VA 22202-4302. Respondents should be aware that notwithstanding any other provision of law, no person shall be subject to any penalty for failing to comply with a collection of information if it does not display a currently valid OMB control number. **PLEASE DO NOT RETURN YOUR FORM TO THE ABOVE ADDRESS.**			

1. REPORT DATE *(DD-MM-YYYY)*	2. REPORT TYPE	3. DATES COVERED *(From - To)*
June 2010	Final	September 2007–August 2009

4. TITLE AND SUBTITLE	5a. CONTRACT NUMBER
Beacon Position and Attitude Navigation Aided by a Magnetometer	W911QX-07-C-0053
	5b. GRANT NUMBER
	5c. PROGRAM ELEMENT NUMBER

6. AUTHOR(S)	5d. PROJECT NUMBER
Xu Ma and Gonzalo R. Arce	08B3K1
	5e. TASK NUMBER
	5f. WORK UNIT NUMBER

7. PERFORMING ORGANIZATION NAME(S) AND ADDRESS(ES)	8. PERFORMING ORGANIZATION REPORT NUMBER
University of Delaware Department of Electrical and Computer Engineering 140 Evans Hall Newark, DE 19716	

9. SPONSORING/MONITORING AGENCY NAME(S) AND ADDRESS(ES)	10. SPONSOR/MONITOR'S ACRONYM(S)
U.S. Army Research Laboratory RDRL-WML-F Aberdeen Proving Ground, MD 21005-5066	ARL-CR-650
	11. SPONSOR/MONITOR'S REPORT NUMBER(S)

12. DISTRIBUTION/AVAILABILITY STATEMENT

Approved for public release; distribution is unlimited.

13. SUPPLEMENTARY NOTES

14. ABSTRACT

Position and attitude estimations are often prerequisites for numerous applications, such as munition systems, mobile robots, and autonomous vehicles. In this report, a position and attitude parameter estimation algorithm suitable for projectiles and microaerial vehicles is developed. The algorithm uses the Earth's magnetic field and a set of fixed beacons as observation vectors. The magnetic field vector observation is obtained from a magnetometer equipped on the object. In addition, a set of angle of arrival vectors is obtained from N-emitting beacons at known ground positions. The algorithm uses iterative, nonlinear object state estimation based on observation vectors to estimate the position and attitude. Position is estimated using the resection algorithm, and attitude is estimated using a two-dimensional direction of arrival estimation algorithm. The proposed method is demonstrated to provide a full position and attitude solution while satisfying the stringent requirements of low-cost and real-time estimation suitable for gun-launched projectiles.

15. SUBJECT TERMS

navigation, attitude, position, estimation, DOA, AOA

16. SECURITY CLASSIFICATION OF:			17. LIMITATION OF ABSTRACT	18. NUMBER OF PAGES	19a. NAME OF RESPONSIBLE PERSON Gary L. Katulka
a. REPORT	**b. ABSTRACT**	**c. THIS PAGE**			**19b. TELEPHONE NUMBER** *(Include area code)*
Unclassified	Unclassified	Unclassified	UU	38	410-306-1071

Contents

List of Figures

Acknowledgments

INTENTIONALLY LEFT BLANK.

1.   Introduction

Position and attitude parameter estimation is often a prerequisite for controlling aerospace mechanical systems moving in space (*1*). Because projectile position often cannot be accurately estimated a priori due to various hardware and environmental uncertainties, guidance, navigation and control (GNC) systems are deployed onboard the object.

Rocket-propelled missile GNC systems are quite mature (*2*, *3*), while effective GNC systems for accurate microunmanned vehicles are under development. For accurate, low-cost, and real-time applications, the design and implementation of the GNC systems are constrained by several technical challenges. Cost is by far the most challenging requirement, while computational efficiency is also required. In addition, robustness is needed in some cases for the desired GNC system to survive extremely harsh environments, such as gun-launched projectiles. Small, compact, and energy-efficient structures are also required for certain applications.

The primary function of position estimation is to locate the coordinates of an object with respect to a set of reference points (*4*). In general, position estimation algorithms can be classified into three groups: methods based on time of arrival (TOA), time difference of arrival (TDOA), and angle of arrival (AOA). TOA methods capture the traveling time of signals between the object and the reference points, from which the distances between them are determined. Subsequently, the position of the object is estimated by the geometric relationship (*5*, *6*). In order to measure the traveling time of signals, TOA systems need the accurate synchronization between the object and the reference points. TDOA methods determine the position of the object by examining the difference in time at which the signal arrives at multiple reference points (*4*). Thus TDOA systems require the accurate synchronization between the reference points. In addition, since the electromagnetic waves propagate at the constant speed of light, both TOA and TDOA systems demand a very high sampling rate to obtain high resolution of the time arrival. Similar to a global positioning system (GPS), the requirements of accurate synchronization and high sampling rate make TOA and TDOA systems expensive. AOA positioning, on the other hand, allows low-cost implementation. It determines the position of an object by the use of the estimated angles between the object and a set of reference points (*7–9*). A variety of algorithms have been proposed to estimate the angle of arrival (*10–17*).

The primary function of the attitude estimation system is to determine the relative orientation between the coordinate frame fixed to the object and another reference coordinate frame (*18*). The attitude of the object can be described in three ways: direction cosine matrix (DCM), quaternion of rotation, and Euler angles (*19*). Wahba (*20*) first addressed the problem of determining the attitude of a rotating body by the vector-matching method. Subsequently, attitude estimation methods have relied mostly on the DCM (*21–23*). When the DCM description is used, the attitude parameters are linearly related to the observed vectors. Thus

linear estimation theory can be applied to the estimation of the DCM. DCM, however, uses nine parameters to describe the attitude, which increases computational complexity. The quaternion of rotation method applies Euler's theorem, which states that any real rotation of one coordinate frame with respect to another may be described by a rotation through some angle about a single fixed axis (*24*). The quaternion method reduces the number of attitude parameters from nine to four. However, the quaternion parameters are nonlinearly related to the observed vectors. Some nonlinear approaches were proposed to determine the quaternion parameters, such as the Quest algorithm and quaternion Kalman filters (*25–27*). The third approach of attitude estimation uses Euler angles. The use of Euler angles is advantageous since the steering commands are explicit functions of the object's Euler angles. In addition, the Euler angle method of attitude estimation requires determining only three parameters. Euler angles, however, are nonlinearly related to the observed vectors, and the attitude tracking using Euler angles is perhaps hampered by possible singularities (*28, 29*). Recently, Wilson (*30*) developed a novel nonlinear approach to estimate the Euler angles of the projectile. However, this proposed system needs three expensive angular rate sensors. Subsequently, Wilson (*31*) extended this work and designed an attitude estimation system only based on a set of magnetometers. This approach, however, requires the exact knowledge of the object's dynamic model with properly modeled forces and moments that sometimes are not observed.

This report proposes a position and attitude navigation system, where both position and attitude can be iteratively estimated based on small and inexpensive sensor devices, such as uniform linear arrays (ULAs) and a magnetometer. It will be explained in section 2.4 that the position or attitude of the object cannot be estimated alone based on N beacons or a magnetometer—both are required. In addition, the algorithm for simultaneously estimating the position and attitude is not robust. Therefore, an iterative position and attitude estimation algorithm is developed in this report. In this iterative algorithm, the position is determined by AOA vector observations, and attitude is tracked using the Euler angle method.

The system is accomplished in several steps. A set of ULAs on the object receiving the impinging RF signals transmitted from ground-based beacons is used to estimate the directions of arrival of the signals. In addition, since the signal-to-noise ratio (SNR) of the magnetometer is usually high, an aiding magnetometer is equipped on the spin axis of the object to improve the performance of the position and attitude estimation. The ULA and magnetometer measurements are exploited to estimate the position of the object based on the prior knowledge of the initial attitude parameters. Based on the position estimation results, the attitude parameters are estimated and updated. The resulting attitude parameter estimates are used to approximate the position parameters in the next estimation cycle. The equations in the algorithms have been developed assuming an ideal vertical magnetic field vector, therefore additional work in the form of coordinate transforms would be required for a generalized solution, which is not specifically addressed in this report. The proposed system is low-cost, and the estimates are simple and thus useful when GPS and expensive inertial measurement units (IMUs) are not available.

The report is organized as follows. The problem formulation is discussed in section 2. The position estimation based on three-dimensional (3-D) AOA location algorithm is developed in section 3. The attitude estimation algorithm based on two-dimensional (2-D) direction of arrival (DOA) estimation is developed in section 4. Simulations of the proposed algorithms are presented in section 5. Section 6 provides conclusions.

2. Problem Formulation

2.1 Coordinate Systems

The motion of an object is usually described by rigid body equations of motion derived from Newton's laws (*29*). This section summarizes and notates three kinds of coordinate systems. The first is the Earth-fixed coordinate system, which is fixed to the Earth with a flat Earth assumption. Denote **X**, **Y**, and **Z** as the unit vectors pointing in the directions of the X, Y, and Z axes, respectively. Without loss of generality, the X, Y, and Z axes point to forward, right, and down, respectively. The second is the body-fixed coordinate system, with three unit vectors $\mathbf{X_b}$, $\mathbf{Y_b}$, and $\mathbf{Z_b}$ pointing to the X_b, Y_b, and Z_b axes, respectively. The X_b axis is along the object's symmetric axis, referred to as the spin axis. The other two axes are perpendicular to the spin axis and each other. The Earth-fixed coordinate system and the body-fixed coordinate system are shown in figure 1. The third is the fixed-plane system, which is a body-fixed system that does not take the spin into account. The three axes are the X_p, Y_p, and Z_p axes, where X_p is overlapped with the X_b axis, and the Y_p axis lies in the horizontal with respect to the Earth.
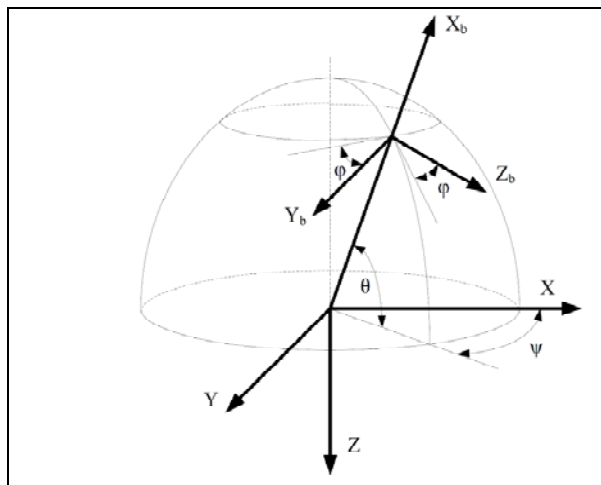

Figure 1. Earth- and body-fixed coordinate systems and
the Euler angle rotations.

The Earth- and body-fixed coordinate systems are related by a Euler rotation sequence. The Earth-fixed system is first rotated about the Z axis through the yaw angle ψ, then about the new Y axis through the pitch angle θ, finally about the new X axis though the roll angle φ, which is shown in figure 1. From the Earth-fixed to body-fixed system, the transformation matrix is

$$T_{eb} = \begin{pmatrix} c_\psi c_\theta & s_\psi c_\theta & -s_\theta \\ c_\psi s_\theta s_\phi - s_\psi c_\phi & s_\psi s_\theta s_\phi + c_\psi c_\phi & c_\theta s_\phi \\ c_\psi s_\theta c_\phi + s_\psi s_\phi & s_\psi s_\theta c_\phi - c_\psi s_\phi & c_\theta c_\phi \end{pmatrix}, \tag{1}$$

where s. is sin($\cdot$) and c. is cos($\cdot$). If the roll angle is fixed as $\varphi = 0$, the transformation matrix from the Earth-fixed to fixed-plane system is

$$T_{ep} = \begin{pmatrix} c_\psi c_\theta & s_\psi c_\theta & -s_\theta \\ -s_\psi & c_\psi & 0 \\ c_\psi s_\theta & s_\psi s_\theta & c_\theta \end{pmatrix}. \tag{2}$$

The transformation matrix from the fixed-plane to body-fixed system is

$$T_{ep} = \begin{pmatrix} 1 & 0 & 0 \\ 0 & c_\psi & s_\phi \\ 0 & -s_\phi & c_\phi \end{pmatrix}. \tag{3}$$

2.2 Beacon Position and Attitude Navigation Aided by Magnetometer

As shown in figure 2, suppose the position of an object is (x_0,y_0,z_0) in 3-D free space and the attitude of the object is (θ, ψ, φ). N beacons are located on the ground at known positions (x_i,y_i,z_i), $i = 1,...,N$, serving as reference points for the position and attitude navigation. The beacons emit RF signals with their antenna patterns spanning 3-D free space. The N signals transmitted from the beacons are represented by the unit vectors of $\vec{s}_1$, $\vec{s}_2$,..., $\vec{s}_N$, each working at frequencies $f_1, f_2,..., f_N$, respectively. The unit vector $\vec{s}_i$ is referred to as the *ith* AOA vector. As shown in figure 2, in the Earth-fixed coordinate, the elevation angles of the AOA vectors are $a_1, a_2,..., a_N$, and the azimuth angles of the AOA vectors are $b_1, b_2,..., b_N$. On the object, N sets of ULAs are equipped to receive impinging signals transmitted from the beacons. In order to distinguish the N signals, these ULAs are applied with different work frequencies of $f_1, f_2,..., f_N$, corresponding to different signals. The structures of the equipped ULAs are shown in figure 3. As shown in figure 3, in the body-fixed coordinate, the elevation angles of the AOA vectors are $\alpha_1, \alpha_2,..., \alpha_N$, and the azimuth angles are $\beta_1, \beta_2,..., \beta_N$. The directivities of the AOA vectors in the Earth-fixed coordinate are described by the elevation and azimuth angles (a_i,b_i), while the directivities of the AOA vectors in the body-fixed coordinate are described by the elevation and azimuth angles (α_i,β_i), where $i = 1, 2,...,N$. In addition, a magnetometer is equipped on the spin axis of the object to measure the magnetic field vector in the body-fixed coordinate. The magnetic field vector in the Earth-fixed coordinate is along the Z-axis in figure 1.
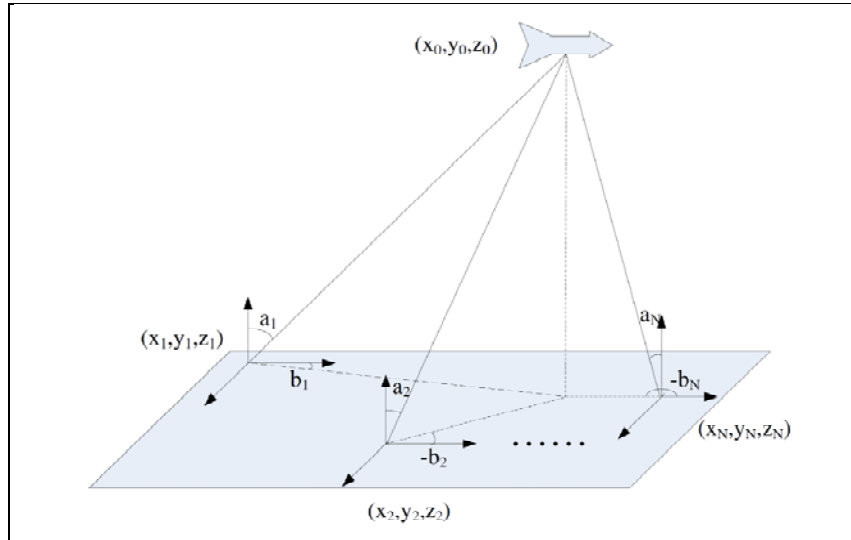
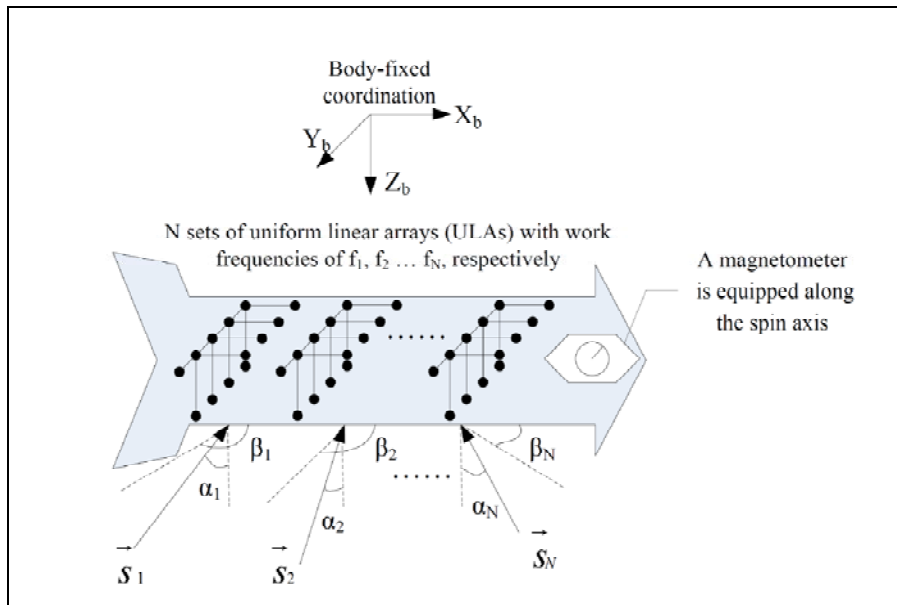Figure 2. Position and attitude estimation based on ground-based beacons.

Figure 3. The ULAs equipped on the object receive the impinging signals.

The voltage measurements from the N sets of ULAs are exploited by a 2-D DOA estimation algorithm, obtaining the estimation of the N pairs of elevation and azimuth angles in the body-fixed coordinate: $(\hat{\alpha}_1, \hat{\beta}_1)$, $(\hat{\alpha}_2, \hat{\beta}_2)$,..., $(\hat{\alpha}_N, \hat{\beta}_N)$. The *ith* pair of the elevation and azimuth angles $(\hat{\alpha}_i, \hat{\beta}_i)$ is referred to as the DOA of the *ith* AOA vector in the body-fixed coordinate. Thus, the ULAs can only measure the AOA vectors in the body-fixed coordinate. In the body-fixed coordinate,

$$\vec{s}_i = (\sin\hat{\alpha}_i \cos\hat{\beta}_i \ \sin\hat{\alpha}_i \sin\hat{\beta}_i \ \cos\hat{\alpha}_i)^T, i = 1, 2, ..., N. \tag{4}$$

On the other hand, in the Earth-fixed coordinate,

$$\vec{s}_i = (\sin a_i \cos b_i \ \sin a_i \sin b_i \ \cos a_i)^T, i = 1, 2, ..., N. \tag{5}$$

A relationship between the AOA vectors in the body-fixed coordinate and in the Earth-fixed coordinate is described as follows. When the transformation relationship between the Earth-fixed and body-fixed coordinates is applied in equation 1,

$$\begin{pmatrix} \sin\hat{\alpha}_i \cos\hat{\beta}_i \\ \sin\hat{\alpha}_i \sin\hat{\beta}_i \\ \cos\hat{\alpha}_i \end{pmatrix} = \begin{pmatrix} c_\psi c_\theta & s_\psi c_\theta & -s_\theta \\ c_\psi s_\theta s_\phi - s_\psi c_\phi & s_\psi s_\theta s_\phi + c_\psi c_\phi & c_\theta s_\phi \\ c_\psi s_\theta c_\phi + s_\psi s_\phi & s_\psi s_\theta c_\phi - c_\psi s_\phi & c_\theta c_\phi \end{pmatrix} \begin{pmatrix} \sin a_i \cos b_i \\ \sin a_i \sin b_i \\ \cos a_i \end{pmatrix}, \tag{6}$$

for $i = 1, 2, ..., N$. Thus, we have

$$\mathbf{u} = \mathbf{H}\mathbf{v}, \tag{7}$$

where

$$\mathbf{u} = [\mathbf{u}_1^T, \mathbf{u}_2^T, ..., \mathbf{u}_N^T]^T \text{ and} \cdots \mathbf{u}_i = (-\sin\hat{\alpha}_i \cos\hat{\beta}_i, -\sin\hat{\alpha}_i \sin\hat{\beta}_i, -\cos\hat{\alpha}_i)^T, \tag{8}$$

$$\mathbf{v} = [\mathbf{v}_1^T, \mathbf{v}_2^T, ..., \mathbf{v}_N^T]^T \text{ and} \cdots \mathbf{v}_i = (\sin a_i \cos b_i, \sin a_i \sin b_i, \cos a_i)^T, i = 1, 2, ..., N, \tag{9}$$

and

$$\mathbf{H} = \begin{pmatrix} \mathbf{T}_{eb1} & 0 & \cdots & 0 \\ 0 & \mathbf{T}_{eb2} & \cdots & 0 \\ \vdots & \ddots & \ddots & \vdots \\ 0 & 0 & \cdots & \mathbf{T}_{ebN} \end{pmatrix}. \tag{10}$$

A transformation of equation 6 is

$$\begin{pmatrix} \sin a_i \cos b_i \\ \sin a_i \sin b_i \\ \cos a_i \end{pmatrix} = \begin{pmatrix} c_\psi c_\theta & s_\psi c_\theta & -s_\theta \\ c_\psi s_\theta s_\phi - s_\psi c_\phi & s_\psi s_\theta s_\phi + c_\psi c_\phi & c_\theta s_\phi \\ c_\psi s_\theta c_\phi + s_\psi s_\phi & s_\psi s_\theta c_\phi - c_\psi s_\phi & c_\theta c_\phi \end{pmatrix}^{-1} \begin{pmatrix} \sin\hat{\alpha}_i \cos\hat{\beta}_i \\ \sin\hat{\alpha}_i \sin\hat{\beta}_i \\ \cos\hat{\alpha}_i \end{pmatrix}, \tag{11}$$

where $i = 1, 2, ..., N$.

2.3 Magnetometer Model

The magnetometer is a device that produces a voltage output proportional to the applied magnetic field in the direction of the magnetometer's sensitive axis. The magnetometer is ideal for broad applications because it is very rugged and low cost. Let the sensitive axis be a unit vector $\mathbf{i}$, and the local magnetic field vector is $\mathbf{B}$. Then the measurement of an ideal magnetometer is the inner product of $\mathbf{i}$ and $\mathbf{B}$

$$M_{ideal} = \mathbf{i} \cdot \mathbf{B} . \tag{12}$$

When the scale and shift influences of the analog circuitry are considered, the actual measurement of the magnetometer is

$$M = s(\mathbf{i} \cdot \mathbf{B}) + b , \tag{13}$$

where s is the scale factor and b is the bias offset. If the included angle between $\mathbf{i}$ and $\mathbf{B}$ is θ, equation 13 is rewritten as

$$M = sB\cos\theta + b , \tag{14}$$

where $B = |\mathbf{B}|$. Thus,

$$\theta = \cos^{-1}\left(\frac{M-b}{sB}\right). \tag{15}$$

In general, the SNR of the magnetometer is very high. However, some amount of noise is always present, which is modeled as white Gaussian noise (WGN). Therefore, the measurement of the magnetometer is adjusted as

$$M = sB\cos\theta + b + n_M, \tag{16}$$

where n_M is WGN with zero mean and a variance of σ^2_M.

2.4 Iterative Position and Attitude Estimation

As described in section 2.2, the proposed navigation system measures one magnetic field vector and N AOA vectors. Based on the measurement vectors, it is proper to ask if these are sufficient to estimate either the position or the attitude. Consider the position estimation first. It will be proven in section 3.2 that three linearly independent vectors in the Earth-fixed coordinate with reference points are necessary and sufficient to determine the position of an object in 3-D free space. Since no reference point is associated to the magnetic field vector, it does not contribute to the estimation of position. Thus, the N AOA vectors must be used in the resection algorithm to estimate the position of the object (7). As mentioned in section 2.2, the ULAs equipped on the object can only measure the AOA vectors in the body-fixed coordinate. In order to obtain the AOA vectors in the Earth-fixed coordinate, the elevation and azimuth angles (a_i,b_i) need to

be estimated from equation 11. In equation 11, the attitude parameters (θ, ψ, φ) are needed to calculated (a_i, b_i). Thus, the position parameters cannot be estimated alone without attitude estimation.

Next, consider the attitude estimation. It has been proven that two pairs of linearly independent vectors are necessary and sufficient to determine the attitude of an object (*21*). That means we have to know the two linearly independent vectors in both the Earth-fixed coordinate and the body-fixed coordinate. As described in section 2.2, the magnetic field vector is known in both coordinates, thus it provides one pair of vectors for the attitude estimation. In order to estimate the attitude parameters, we need to find another pair of linearly independent vectors from the *N* AOA vectors. Although the ULAs measure the AOA vectors in the body-fixed coordinate, we cannot obtain the AOA vectors in the Earth-fixed coordinate without the position of the object. Thus, we cannot find another pair of linearly independent vectors without position estimation. In an attitude estimation system, position information is usually obtained by GPS (*18*). Based on the previous analysis, the position or attitude cannot be estimated alone.

Given that the position and attitude must be estimated jointly, the next question to address is if the position and attitude can be estimated simultaneously. The magnetometer measurement is shown in equation 16. The ULA measurements are described in equation 6, which can be rewritten as

$$
\begin{pmatrix} \sin\hat{\alpha}_i \cos\hat{\beta}_i \\ \sin\hat{\alpha}_i \sin\hat{\beta}_i \\ \cos\hat{\alpha}_i \end{pmatrix} = \begin{pmatrix} c_\psi c_\theta & s_\psi c_\theta & -s_\theta \\ c_\psi s_\theta s_\phi - s_\psi c_\phi & s_\psi s_\theta s_\phi + c_\psi c_\phi & c_\theta s_\phi \\ c_\psi s_\theta c_\phi + s_\psi s_\phi & s_\psi s_\theta c_\phi - c_\psi s_\phi & c_\theta c_\phi \end{pmatrix} \begin{pmatrix} (x_i - x_0)/norm_i \\ (y_i - y_0)/norm_i \\ (z_i - z_0)/norm_i \end{pmatrix},
\tag{17}
$$

where $norm_i = \{ (x_i - x_0)^2 + (y_i - y_0)^2 + (z_i - z_0)^2 \}^{1/2}$. Thus, equations 16 and 17 consist of a system of equations, where $\mathbf{m} = (x_0, y_0, z_0, \theta, \psi, \varphi)^T$ are the unknown position and attitude parameters to be estimated. Equations 16 and 17 are nonlinear equations, where the unknown parameters are coupled together. In the simultaneous position and attitude estimation process, the parameter vector $\mathbf{m}$ must be estimated using recursive algorithms, such as a nonlinear least squares estimation algorithm. Our extensive simulations show that these simultaneous position and attitude estimation algorithms are not robust. If the SNR of the ULAs is smaller than 25 dB, the algorithm exploiting four beacons does not converge with very high probability.

While the simultaneous position and attitude estimation is not robust, iterative position and attitude estimation algorithms are proposed next based on beacons and a magnetometer. Suppose the initial attitude of the object before launch is known as ($\theta^*, \psi^*, \varphi^*$). At the beginning of the estimation process, the initial attitude parameters of (φ, ψ, θ) are used to solve the elevation and azimuth angles ($\hat{\alpha}_i, \hat{b}_i$) according to equation 9. Based on the estimation results of ($\hat{\alpha}_i, \hat{b}_i$), the position of ($x_0, y_0, z_0$) can be subsequently estimated based on the 3-D AOA location algorithm proposed in section 3.2. Based on equations 16 and 17 and the position estimation

results, the attitude parameters of (θ, ψ, φ) can be updated by the nonlinear estimation approach proposed in section 4.2. Then the current attitude estimation results will be exploited to update $(\hat{a}_i, \hat{b}_i)$ in the next iteration. The scheme of the iterative position and attitude estimation algorithms is illustrated in figure 4. The details of the position and attitude estimation algorithm are presented in sections 3 and 4.
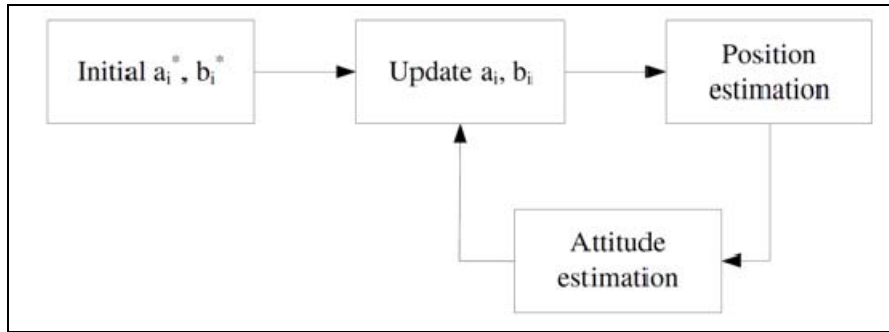

Figure 4. Iterative position and attitude estimation algorithm based on beacons and a magnetometer.

In section 3.2, it is shown that three AOA vectors are necessary and sufficient to determine the position of the object. In the appendix, it is shown geometrically that two AOA vectors are necessary and sufficient to determine the attitude of the object. Therefore, in order to estimate both position and attitude, the proposed algorithms use three ground-based beacons. Since the magnetometer has very high SNR, an aiding magnetometer measures an additional magnetic field vector to improve the performance of the position and attitude estimation.

3. Position Estimation Based on 3-D AOA Vectors

3.1 2-D AOA Location Algorithm

In this section, the 2-D AOA location algorithm will be first summarized and exploited as the foundation of the proposed 3-D AOA location algorithm. The 2-D AOA position algorithm, referred to as the resection algorithm, was proposed by Rappaport et al. (*4*) and McGillem and Rappaport (*7*). The coordinates for the analytic geometry solution of the AOA position location are shown in figure 5, where the position of points A, B, and C are (x_1, y_1), (x_2, y_2), and (x_3, y_3), respectively. The angle between $\overline{AP}$ and $\overline{BP}$ is γ_1. The angle between $\overline{BP}$ and $\overline{CP}$ is γ_2. The angle between $\overline{AB}$ and the horizontal direction is τ_1. The angle between $\overline{BC}$ and the horizontal direction is τ_2. Let the position of P be (x_0, y_0), which is calculated based on the following known parameters:
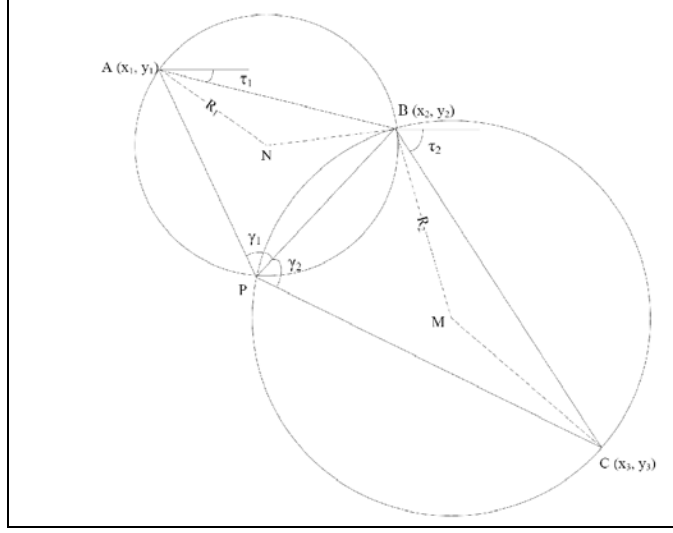
Figure 5. Coordinates for the analytic geometry solution of the 2-D AOA position location.

$$y_0 = \frac{2mx_N + 2y_N - 2mn}{1 + m^2} - y_2 \tag{18}$$

and

$$x_0 = my_0 + n \,, \tag{19}$$

where

$$m = \frac{y_M - y_N}{x_N + x_M} \,, \tag{20}$$

$$n = \frac{R_2^2 - R_1^2 - x_M^2 + x_N^2 - y_M^2 + y_N^2}{2(x_N + x_M)} \,, \tag{21}$$

$$x_N = x_1 - R_1 \sin(\tau_1 - \gamma_1) \,, \tag{22}$$

$$y_N = y_1 - R_1 \cos(\tau_1 - \gamma_1) \,, \tag{23}$$

$$x_M = x_2 - R_2 \sin(\tau_2 - \gamma_2) \,, \tag{24}$$

$$y_M = x_2 - R_2 \cos(\tau_2 - \gamma_2) \,, \tag{25}$$

$$R_1 = \frac{\overline{AB}}{2 \sin \gamma_1} \,, \tag{26}$$

and

$$R_2 = \frac{\overline{BC}}{2\sin\gamma_2} \ . \tag{27}$$

For the case of $x_0 = my_0 + n$, equations 18 and 19 maybe equivalently expressed as

$$x_0 = \frac{2m' y_N + 2x_N + 2m' n'}{1 + m'^2} - x_2 \tag{28}$$

and

$$y_0 = m' x_0 - n' \ , \tag{29}$$

where $m' = \dfrac{1}{m}$ and $n' = \dfrac{n}{m}$.

3.2   Position Estimation Based on 3-D AOA Measurements

In this section, a 3-D AOA location algorithm is generalized from the 2-D AOA location algorithm described in section 3.1. It is noted that the resection algorithm requires at least three AOA vectors to solve for the location in two dimensions. Suppose three beacons at known positions are available. It will be shown in the following section that the three beacons are sufficient to solve for the location in three dimensions, if the attitude of the object is assumed to be known as $(\hat{\theta},\hat{\psi},\hat{\phi})$. In order to estimate the position of the object in 3-D free space, the 3-D coordinates are first projected into the 2-D X-Y plane, as illustrated in figure 6, where the three beacons are located at points $A(x_1,y_1)$, $B(x_2,y_2)$, and $C(x_3,y_3)$, respectively. The position of the object in the X-Y plane is $P(x_0,y_0)$. The included angle between $\overline{AP}$ and $\overline{BP}$ is $|b_2 - b_1|$, and the included angle between $\overline{BP}$ and $\overline{CP}$ is $|b_3 - b_2|$, where b_1, b_2, and b_3 are the azimuth angles of $\vec{s}_1$, $\vec{s}_2$, and $\vec{s}_3$ in the Earth-fixed coordinate, respectively. However, when the position of the object is unknown, b_1, b_2, and b_3 cannot be determined. Therefore, b_1, b_2, and b_3 need to be estimated from the attitude estimation results. According to equation 11, we have

$$\begin{pmatrix} \sin\hat{a}_i \cos\hat{b}_i \\ \sin\hat{a}_i \sin\hat{b}_i \\ \cos\hat{a}_i \end{pmatrix} = \begin{pmatrix} \hat{s}_{i1} \\ \hat{s}_{i2} \\ \hat{s}_{i3} \end{pmatrix} = \begin{pmatrix} c_{\hat{\psi}}c_{\hat{\theta}} & s_{\hat{\psi}}c_{\hat{\theta}} & -s_{\hat{\theta}} \\ c_{\hat{\psi}}s_{\hat{\theta}}s_{\hat{\phi}} - s_{\hat{\psi}}c_{\hat{\phi}} & s_{\hat{\psi}}s_{\hat{\theta}}s_{\hat{\phi}} + c_{\hat{\psi}}c_{\hat{\phi}} & c_{\hat{\theta}}s_{\hat{\phi}} \\ c_{\hat{\psi}}s_{\hat{\theta}}c_{\hat{\phi}} + s_{\hat{\psi}}s_{\hat{\phi}} & s_{\hat{\psi}}s_{\hat{\theta}}c_{\hat{\phi}} - c_{\hat{\psi}}s_{\hat{\phi}} & c_{\hat{\theta}}c_{\hat{\phi}} \end{pmatrix}^{-1} \begin{pmatrix} \sin\hat{\alpha}_i \cos\hat{\beta}_i \\ \sin\hat{\alpha}_i \sin\hat{\beta}_i \\ \cos\hat{\alpha}_i \end{pmatrix} , \tag{30}$$
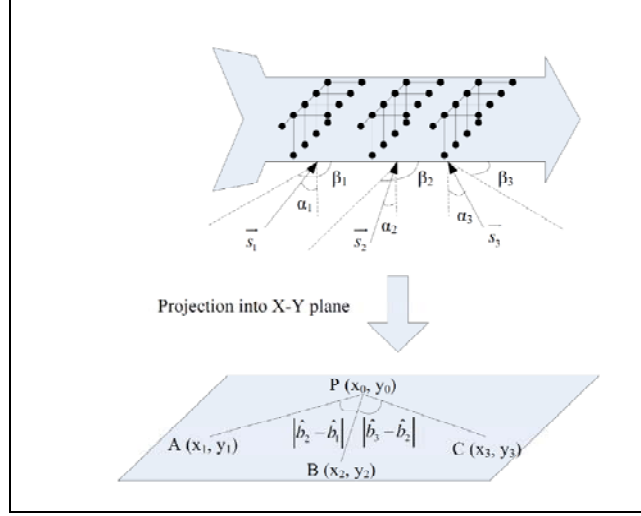
Figure 6. The 3-D coordinates are projected into the 2-D
X-Y plane.

where $i = 1, 2, 3$. In equation 30, $\hat{\theta}$, $\hat{\psi}$, and $\hat{\phi}$ are the attitude estimation results, and $\hat{\alpha}_i$ and $\hat{\beta}_i$ are the estimation of elevation and azimuth angles of $\vec{s}_i$ in the body-fixed coordinate, obtained from the fast 2-D DOA estimation algorithm described in section 4.1. According to equation 30, a_i and b_i are estimated as follows:

$$\hat{a}_i = \cos^{-1}(\hat{s}_{i3}) \tag{31}$$

and

$$\hat{b}_i = \begin{cases} \tan^{-1}(\hat{s}_{i2}/\hat{s}_{i1}) & : & \dfrac{\hat{s}_{i2}}{\sin \hat{a}_i} > 0 \oplus \dfrac{\hat{s}_{i1}}{\sin \hat{a}_i} > 0 \\[2ex] \tan^{-1}(\hat{s}_{i2}/\hat{s}_{i1}) + 2\pi & : & \dfrac{\hat{s}_{i2}}{\sin \hat{a}_i} < 0 \oplus \dfrac{\hat{s}_{i1}}{\sin \hat{a}_i} > 0 \\[2ex] \tan^{-1}(\hat{s}_{i2}/\hat{s}_{i1}) + \pi & : & \text{otherwise} \end{cases} \tag{32}$$

These parameters are applied for the resection algorithm described in section 3.1 to estimate $\hat{x}_0$ and $\hat{y}_0$, where $\gamma_1 = \left| \hat{b}_2 - \hat{b}_1 \right|$, $\gamma_2 = \left| \hat{b}_3 - \hat{b}_2 \right|$, $\tau_1 = \tan^{-1}\left(\left| \dfrac{y_2 - y_1}{x_2 - x_1} \right| \right)$ and $\tau_2 = \tan^{-1}\left(\left| \dfrac{y_3 - y_2}{x_3 - x_2} \right| \right)$.

In addition, the altitude of the object z_0 may be estimated from the geometric relationship

12

$$\tan^2 \hat{a}_i = \frac{(\hat{x}_0 - x_i)^2 + (\hat{y}_0 - y_i)^2}{(\hat{z}_0 - z_i)^2} \ . \tag{33}$$

Thus

$$\hat{z}_{0i} = z_i + \sqrt{\frac{(\hat{x}_0 - x_i)^2 + (\hat{y}_0 - y_i)^2}{\tan^2 \hat{a}_i}} \ , \tag{34}$$

where $i = 1, 2, 3$. When the mean estimation is applied, $\hat{z}_0$ can be estimated as

$$\hat{z}_o = \frac{1}{3} \sum_{i=1}^{3} \hat{z}_{oi} \ . \tag{35}$$

Therefore, three beacons are necessary and sufficient to estimate the position of the object in 3-D free space.

4. Attitude Estimation Algorithm Based on 2-D DOA Estimation

4.1 A Fast 2-D DOA Estimation Algorithm

Several 2-D DOA estimation algorithms have been presented in the literature. Maximum likelihood methods with high computational complexity were first proposed (*10, 11*). MUSIC and ESPRIT algorithms exploited either eigen value decomposition or singular value decomposition to obtain high resolution in DOA estimation (*12–15*). Wu et al. (*16*) proposed a 2-D DOA estimation algorithm based on propagator method. Recently, Tayem and Kwon (*17*) proposed a computationally efficient azimuth and elevation angle estimation algorithm with no failure and no eigen decomposition. The computational efficiency and accuracy of this algorithm are suitable for the real-time estimation of a rapidly moving object. This fast 2-D DOA estimation algorithm is summarized in the appendix. It will be exploited to formulate the position and attitude estimation algorithms.

Figure 7 shows the proposed array configuration consisting of three ULAs with interspacing d equal to a half wavelength of incident signals. The three ULAs consist of N, $N+1$, and N elements, respectively. The first and third ULAs are referred to as subarrays Z and W, respectively. The first and last N elements in the second ULA are referred to as subarrays X and Y, respectively. Thus, subarrays X, Y, Z, and W consist of N elements. Suppose there are K narrow-band sources, $s(t) = [s_1(t), s_2(t), ..., s_K(t)]^T$, with the same wavelength λ impinging on the arrays. The received signals at the subarrays X, Y, Z, and W are
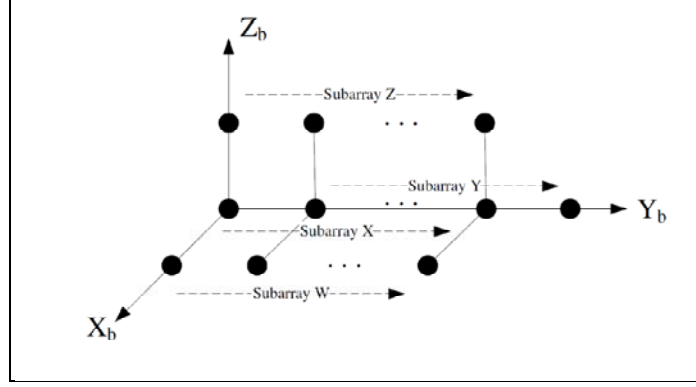
Figure 7. The proposed array configuration equipped on the object.

$$x(t)= \mathbf{A}s(t) + \mathbf{n}_x(t) ,$$

$$y(t)= \mathbf{A}\mathbf{\Phi}_y s(t) + \mathbf{n}_y(t) ,$$

$$z(t)= \mathbf{A}\mathbf{\Phi}_z s(t) + \mathbf{n}_z(t) ,$$

$$w(t)= \mathbf{A}\mathbf{\Phi}_w s(t) + \mathbf{n}_w(t) ,$$

$$t =1, 2, \ldots , L , \tag{36}$$

where

$$\mathbf{A} = [\mathbf{a}(\alpha_1, \beta_1) , a(\alpha_2, \beta_2), \ldots, \mathbf{a}(\alpha_K, \beta_K)] , \tag{37}$$

$$\mathbf{a}(\alpha_k, \beta_k) = \left[1, \exp\left(-j\frac{2\pi d \sin \alpha_k \sin \beta_k}{\lambda} \right), \ldots, \exp\left(-j\frac{2(N-1)\pi d \sin \alpha_k \sin \beta_k}{\lambda} \right) \right]^T , \tag{38}$$

$$\Phi_y = \mathrm{diag}[p_1, p_2, \ldots, p_K] , \text{ where } p_K = \exp\left(-j\frac{2\pi d \sin \alpha_k \sin \beta_k}{\lambda} \right) , \tag{39}$$

$$\Phi_z = \mathrm{diag}[q_1, q_2, \ldots, q_K] , \text{ where } q_K = \exp\left(-j\frac{2\pi d \cos \alpha_k}{\lambda} \right) , \tag{40}$$

$$\Phi_w = \mathrm{diag}[r_1, r_2, \ldots, r_K] , \text{ where } r_K = \exp\left(-j\frac{2\pi d \sin \alpha_k \cos \beta_k}{\lambda} \right) , \tag{41}$$

where $k = 1, 2,\ldots,K$. Let $\mathbf{g}(t) = [\mathbf{x}^T(t), \mathbf{y}^T(t), \mathbf{z}^T(t), \mathbf{w}^T(t)]^T$ denote a $4N \times 1$ snapshot data vector with $t = 1, 2,\ldots,L$. Let $\mathbf{F} = [\mathbf{g}(1), \mathbf{g}(2),\ldots, \mathbf{g}(L)]$ denote a $4N \times L$ data matrix consisting of L snapshots. The partition of $\mathbf{F}$ is $\mathbf{F} = [\mathbf{F}_1^T, \mathbf{F}_2^T]^T$, where $\mathbf{F}_1$ and $\mathbf{F}_2$ are submatrices with dimensions of $K \times L$ and $(4N - K) \times L$, respectively. Let $\hat{\mathbf{P}} = (\mathbf{F}_1\mathbf{F}_1^H)^{-1}\mathbf{F}_1\mathbf{F}_2^H$ denote the $K \times (4N - K)$ propagator estimate matrix based on the data matrix $\mathbf{F}$. The partitions of $\hat{\mathbf{P}}$ are

14

$\hat{\mathbf{P}}^{H \, \hat{}\, H} = [\hat{P}_1^T, \hat{P}_2^T, \hat{P}_3^T, \hat{P}_4^T, \hat{P}_5^T, \hat{P}_6^T, \hat{P}_7^T]^T$, where the dimension of $\hat{P}_1^T, \hat{P}_3^T, \hat{P}_5^T$ and $\hat{P}_7^T$ is $(N-K) \times K$, and the dimension of $\hat{P}_2^T, \hat{P}_4^T$, and $\hat{P}_6^T$ is $K \times K$. Thus, the diagonal elements of $\mathbf{\Phi}_y, \mathbf{\Phi}_z$, and $\mathbf{\Phi}_w$, respectively, can be estimated by finding the K eigen values of $\hat{P}_3 \hat{P}_1^{\#}, \hat{P}_5 \hat{P}_1^{\#}$ and $\hat{P}_7 \hat{P}_1^{\#}$, where # denotes the pseudoinverse. Finally, the azimuth and elevation angles for each source can be estimated as

$$\hat{\beta}_k = \tan^{-1}\left[\frac{\arg(\mathbf{\Phi}_y)_{kk}}{\arg(\mathbf{\Phi}_w)_{kk}}\right], \qquad k = 1, 2, \ldots, K. \tag{42}$$

$$\hat{\alpha}_k = \tan^{-1}\left[\frac{\arg(\mathbf{\Phi}_w)_{kk}}{\arg(\mathbf{\Phi}_z)_{kk} \cos \hat{\beta}_k}\right], \qquad k = 1, 2, \ldots, K. \tag{43}$$

4.2 Attitude Estimation Algorithm Based on Fast 2-D DOA Estimation

In this section, an attitude estimation algorithm is proposed based on the fast 2-D DOA estimation described in section 4.1. Suppose one magnetometer is equipped on the spin axis of the object. According to equation 15, and assuming $b = 0$ and $sB = 1$, the pitch angle (assuming a vertical magnetic field vector) is estimated as

$$\hat{\theta} = -\sin^{-1}(M), \tag{44}$$

where M is the measurement of the magnetometer.

On the other hand, it has been proven that two pairs of linearly independent vectors are necessary and sufficient to determine the attitude of the object (*21*). That means that given the position of the object, two ground-based beacons are necessary and sufficient to determine the attitude. The appendix gives a geometric explanation for this. Our proposed navigation system includes three beacons that are redundant to estimate the attitude. Corresponding to the three beacons, three sets of ULAs are equipped on the object to receive impinging signals. As described in section 3.2, the current position parameters have already been estimated as $(\hat{x}_0, \hat{y}_0, \hat{z}_0)$. Let the positions of the three beacons be (x_1, y_1, z_1), (x_2, y_2, z_2), and (x_3, y_3, z_3), respectively. Based on equation 17, we have

$$\begin{pmatrix} \sin \hat{\alpha}_i \cos \hat{\beta}_i \\ \sin \hat{\alpha}_i \sin \hat{\beta}_i \\ \cos \hat{\alpha}_i \end{pmatrix} = \begin{pmatrix} c_\psi c_{\hat{\theta}} & s_\psi c_{\hat{\theta}} & -s_{\hat{\theta}} \\ c_\psi s_{\hat{\theta}} s_\phi - s_\psi c_\phi & s_\psi s_{\hat{\theta}} s_\phi + c_\psi c_\phi & c_{\hat{\theta}} s_\phi \\ c_\psi s_{\hat{\theta}} c_\phi + s_\psi s_\phi & s_\psi s_{\hat{\theta}} c_\phi - c_\psi s_\phi & c_{\hat{\theta}} c_\phi \end{pmatrix} \begin{pmatrix} (x_i - \hat{x}_0)/\widehat{norm}_i \\ (y_i - \hat{y}_0)/\widehat{norm}_i \\ (z_i - \hat{z}_0)/\widehat{norm}_i \end{pmatrix}, \tag{45}$$

where $\widehat{norm}_i = \{(x_i - \hat{x}_0)^2 + (y_i - \hat{y}_0)^2 + (z_i - \hat{z}_0)^2\}1/2$ and $i = 1, 2, 3$. Thus, we have

$$\mathbf{u} = \mathbf{Hv}, \tag{46}$$

where

$$\mathbf{u} = [\mathbf{u}_1^T, \mathbf{u}_2^T, ..., \mathbf{u}_N^T]^T \text{ and} \cdots \mathbf{u}_i = (-\sin\hat{\alpha}_i \cos\hat{\beta}_i, -\sin\hat{\alpha}_i \sin\hat{\beta}_i, -\cos\hat{\alpha}_i)^T , \qquad (47)$$

$$\mathbf{v} = [\mathbf{v}_1^T, \mathbf{v}_2^T, ..., \mathbf{v}_N^T]^T \text{ and} \cdots \mathbf{v}_i = (\sin a_i \cos b_i, \sin a_i \sin b_i, \cos a_i)^T , i = 1, 2, ..., N , \qquad (48)$$

and

$$\mathbf{H} = \begin{pmatrix} \mathbf{T}_{eb} & 0 & 0 \\ 0 & \mathbf{T}_{eb} & 0 \\ 0 & 0 & \mathbf{T}_{eb} \end{pmatrix} , \qquad (49)$$

Let $\hat{s}_{i1} = \dfrac{x_i - \hat{x}_0}{norm_i}$, $\hat{s}_{i2} = \dfrac{y_i - \hat{y}_0}{norm_i}$, and $\hat{s}_{i3} = \dfrac{z_i - \hat{z}_0}{norm_i}$. From the first equation of equation 45, we have

$$\cos(\psi_i - \gamma_i) = \frac{\sin\hat{\alpha}_i \cos\hat{\beta}_i + s_{\hat{\theta}} \hat{s}_{i3}}{c_{\hat{\theta}}} , \qquad (50)$$

where γ can be estimated as

$$\hat{\gamma}_i = \begin{cases} \tan^{-1}(\hat{s}_{i2}/\hat{s}_{i1}) & : & \dfrac{\hat{s}_{i2}}{\sqrt{\hat{s}_{i1}^2 + \hat{s}_{i2}^2}} > 0 \oplus \dfrac{\hat{s}_{i2}}{\sqrt{\hat{s}_{i1}^2 + \hat{s}_{i2}^2}} > 0 \\[3ex] \tan^{-1}(\hat{s}_{i2}/\hat{s}_{i1}) + 2\pi & : & \dfrac{\hat{s}_{i2}}{\sqrt{\hat{s}_{i1}^2 + \hat{s}_{i2}^2}} < 0 \oplus \dfrac{\hat{s}_{i2}}{\sqrt{\hat{s}_{i1}^2 + \hat{s}_{i2}^2}} < 0 \\[3ex] \tan^{-1}(\hat{s}_{i2}/\hat{s}_{i1}) + \pi & : & \text{otherwise} \end{cases} . \qquad (51)$$

Since the range of $\hat{\psi}_i - \hat{\gamma}_i$ is unknown, $\hat{\psi}_i$ cannot be uniquely estimated from equation 50. The estimation $\hat{\psi}_i$ from the last iteration then provides an estimate of the range of $\hat{\psi}_i - \hat{\gamma}_i$. Let $\hat{\psi}_i^k$ be the estimation result of ψ_i in the kth iteration. Then in the $k + 1^{th}$ iteration,

$$\hat{\psi}_i^{k+1} = \begin{cases} \hat{\gamma}_i - 2\pi + \Delta & : & \hat{\psi}_i^k - \hat{\gamma}_i \in [-2\pi, -\pi] \\ \hat{\gamma}_i - \Delta & : & \hat{\psi}_i^k - \hat{\gamma}_i \in [-\pi, 0] \\ \hat{\gamma}_i + \Delta & : & \hat{\psi}_i^k - \hat{\gamma}_i \in [0, \pi] \\ \hat{\gamma}_i + 2\pi - \Delta & : & \hat{\psi}_i^k - \hat{\gamma}_i \in [\pi, 2\pi] \end{cases} , \qquad (52)$$

where

16

$$\Delta = \cos^{-1}\left(\frac{\sin\hat{\alpha}_i \cos\hat{\beta}_i + s_{\hat{\theta}}\hat{s}_{i3}}{c_{\hat{\theta}}}\right). \tag{53}$$

Averaging over the three sets of estimations, we have

$$\hat{\psi} = \frac{1}{3}\sum_{i=1}^{3}\hat{\psi}_i . \tag{54}$$

From the second and third equations of equation 45, we have

$$\begin{aligned}\sin\hat{\alpha}_i \cos\hat{\beta}_i &= m_1 \sin\phi + m_2 \cos\phi \\ \cos\hat{\alpha}_i &= m_3 \sin\phi + m_4 \cos\phi\end{aligned}, \tag{55}$$

where

$$\begin{aligned}m_1 &= \sin\hat{a}_i \cos\hat{b}_i c_{\hat{\psi}} s_{\hat{\theta}} + \sin\hat{a}_i \sin\hat{b}_i s_{\hat{\psi}} s_{\hat{\theta}} + \cos\hat{a}_i c_{\hat{\theta}} \\ m_2 &= \sin\hat{a}_i \sin\hat{b}_i c_{\hat{\psi}} - \sin\hat{a}_i \cos\hat{b}_i s_{\hat{\psi}} \\ m_3 &= \sin\hat{a}_i \cos\hat{b}_i s_{\hat{\psi}} - \sin\hat{a}_i \sin\hat{b}_i c_{\hat{\psi}} \\ m_4 &= \sin\hat{a}_i \cos\hat{b}_i c_{\hat{\psi}} s_{\hat{\theta}} + \sin\hat{a}_i \sin\hat{b}_i s_{\hat{\psi}} s_{\hat{\theta}} + \cos\hat{a}_i c_{\hat{\theta}}\end{aligned}. \tag{56}$$

Thus, for each i, $\sin\hat{\phi}_i$ and $cis\hat{\phi}_i$ can be solved as

$$\sin\hat{\phi}_i = \frac{-m_4 \sin\hat{\alpha}_i \sin\hat{\beta}_i - m_2 \cos\hat{\alpha}_i}{m_1 m_4 - m_2 m_3}. \tag{57}$$

$$\cos\hat{\phi}_i = \frac{-m_3 \sin\hat{\alpha}_i \sin\hat{\beta}_i - m_1 \cos\hat{\alpha}_i}{m_2 m_3 - m_1 m_4}. \tag{58}$$

Therefore,

$$\hat{\phi}_i = \begin{vmatrix}\tan^{-1}(\sin\hat{\phi}_i / \cos\hat{\phi}_i) & : & \sin\hat{\phi}_i > 0 \oplus \cos\hat{\phi}_i > 0 \\ \tan^{-1}(\sin\hat{\phi}_i / \cos\hat{\phi}_i) + 2\pi & : & \sin\hat{\phi}_i < 0 \oplus \cos\hat{\phi}_i < 0 \\ \tan^{-1}(\hat{s}_{i2} / \hat{s}_{i1}) + \pi & : & otherwise\end{vmatrix}. \tag{59}$$

Applying an averaging operation over the three sets of estimations, we have

$$\hat{\phi} = \frac{1}{3}\sum_{i=1}^{3}\hat{\phi}_i . \tag{60}$$

5. Simulations

5.1 Performance-Enhancement Techniques

In section 4.2, equations 54 and 60 are intended to give good estimations of the yaw and roll angles, respectively. However, when the denominators in equations 50 and 57–59 are small, the errors of the estimations are magnified. In addition, in the iterative position and attitude estimation algorithms, the error may be transferred between each other and accumulated. In order to further improve the estimation performance, a recursive median filter is applied in the estimation process to remove large deviations from the estimation results (*32*). The output of the recursive median filter with window width equal to $2N+1$ is

$$\hat{x}_M(t) = median\left[\hat{x}_M(t-N\varDelta t),...,\hat{x}_M(t-\varDelta t),\hat{x}(t),\hat{x}(t+\varDelta t),...,\hat{x}_M(t+N\varDelta t)\right], \tag{61}$$

where $\hat{x}$ is the arbitrary estimated parameter and $\varDelta t$ is the sampling interval. In the recursive median filter, the prior outputs are used in the current filter step. As shown in equation 61, $\hat{x}_M(t-N\varDelta t),...,\hat{x}_M(t-\varDelta t)$ are prior outputs. Since the SNR of the magnetometer is usually very high, the recursive median filter is not applied to the estimation of the pitch angle.

5.2 Simulations of Iterative Position and Attitude Estimation Algorithms

The proposed iterative position and attitude estimation algorithms are simulated using a gun-launched object. In these simulations, the object is launched with an initial pitch angle $\theta_0 = 45°$, initial yaw angle $\psi_0 = 0°$, initial roll angle $\varphi_0 = 0°$, and initial position at (0, 0, 0). The trajectory of the object is a standard parabola. The range of the trajectory is 3 km and the traveling time is 2 s. Three ground-based beacons are located at (–1500, 3000, 0), (4000, 1000, 0), and (6000, –4000, 0), respectively. The work frequencies of the three beacons are $f_1 = 10$ GHz, $f_2 = 5$ GHz, and $f_3 = 7.5$ GHz, respectively. All the subarrays of the ULAs equipped on the object consist of $N = 4$ elements. Assume the noise on the ULAs is WGN, with SNR = 20 dB. The noise on the magnetometer is also WGN, with the variance $\sigma^2_M = 10^{-6}$.

The relative locations between the trajectory of the object and the three beacons are illustrated in figure 8. Recursive median filters with window width equal to 7 are applied to the estimations of ψ, φ, x_0, y_0, and z_0. The simulation results are shown in figures 9–14, corresponding to the estimations of coordinates on the X-axis, Y-axis, Z-axis, and pitch angle, yaw angle and roll angle, respectively.
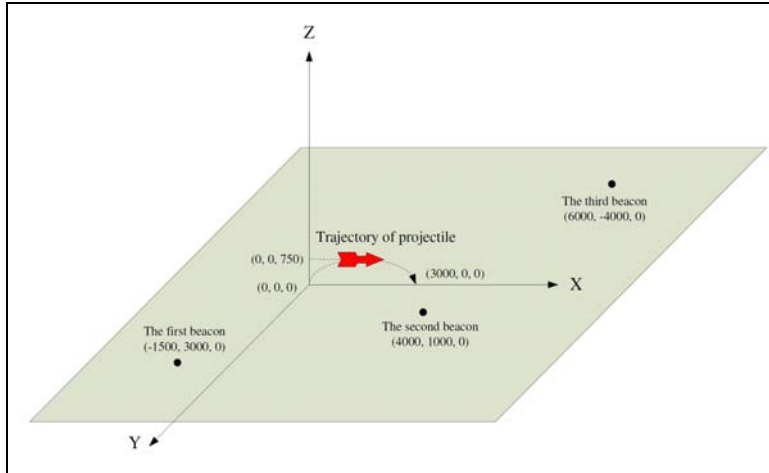
Figure 8. Relative locations between the trajectory of the object and the
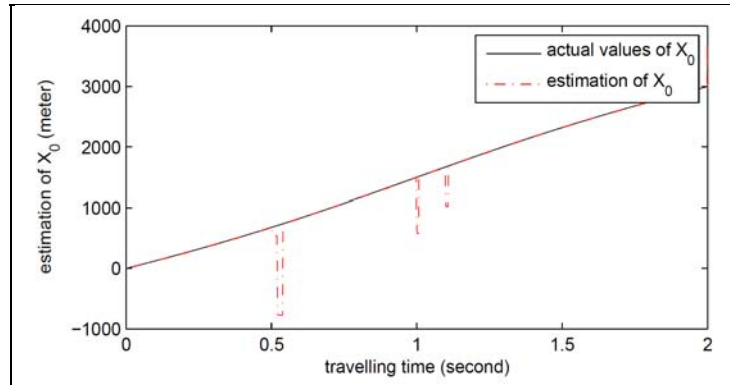three beacons.

Figure 9. Simulation result for the estimation of x_0. SNR = 20 dB.
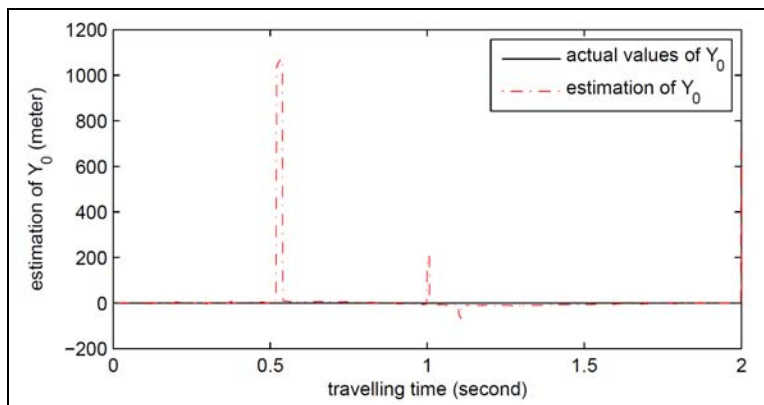$MSE = 2.63 \times 10^4$.

Figure 10. Simulation result for the estimation of y_0. SNR = 20 dB.
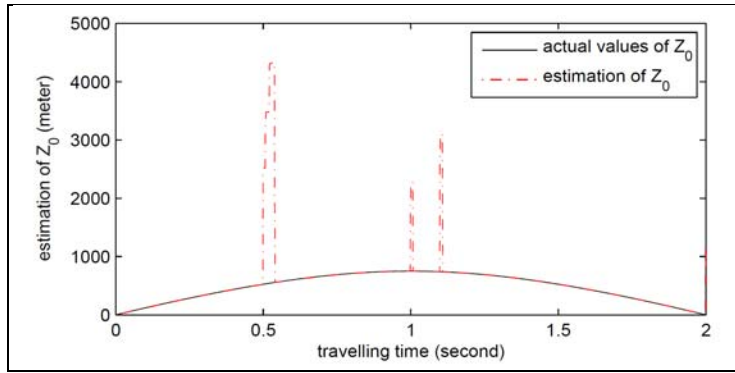$MSE = 1.11 \times 10^4$.

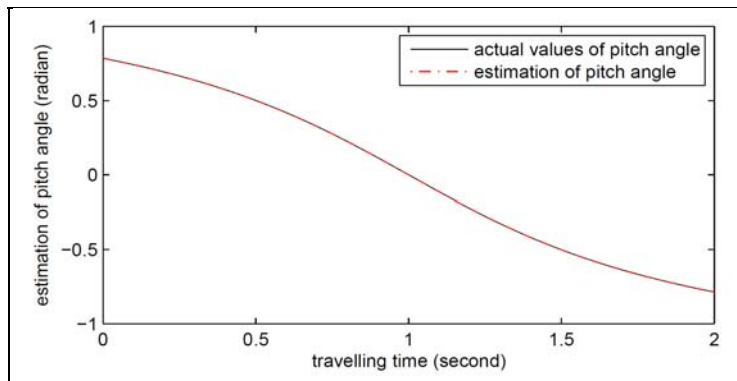Figure 11. Simulation result for the estimation of z_0. SNR = 20 dB. MSE = 2.37×10^5.

Figure 12. Simulation result for the estimation of pitch angle. SNR = 20 dB. MSE = 1.31×10^{-6}.

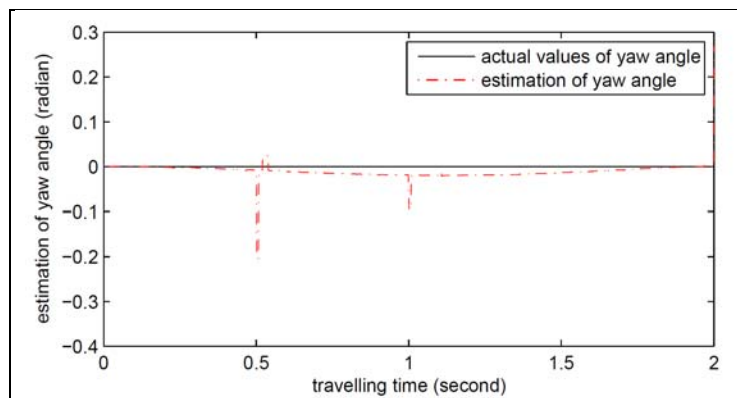

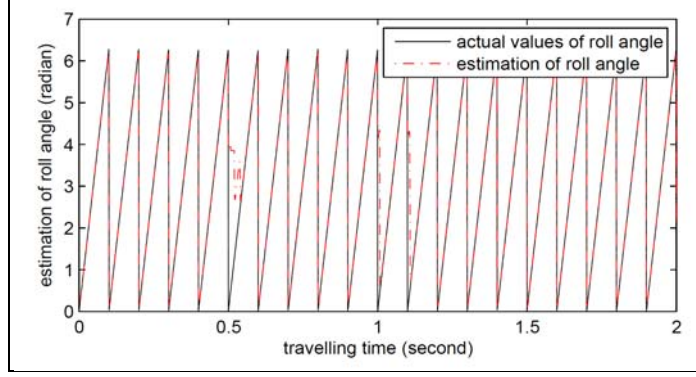Figure 13. Simulation result for the estimation of yaw angle. SNR = 20 dB. MSE = 3.37×10^{-4}.

Figure 14. Simulation result for the estimation of roll angle.
SNR = 20 dB. MSE = 2.97×10^{-1}.

In figures 9–14, the MSE of $\hat{x}_0$ is 2.63×10^4, the MSE of $\hat{y}_0$ is 1.11×10^4, the MSE of $\hat{z}_0$ is 2.37×10^5, the MSE of $\hat{\theta}$ is 1.31×10^{-6}, the MSE of $\hat{\psi}$ is 3.37×10^{-4}, and the MSE of $\hat{\phi}$ is 2.97×10^{-1}. The recursive median filters successfully remove some large deviations from the estimation results. However, it is noted that there are still some singular points in figures 9–11, 13, and 14, which result in the large MSEs of $\hat{x}_0$, $\hat{y}_0$, and $\hat{z}_0$. There are two reasons for the singularity. First, the denominators in equations 57–59 are close to zero. Second, the use of $\hat{\phi}_i^k$ to guess the range of $\hat{\phi}_i^{k+1} - \hat{\gamma}_i$ in equation 52 can sometimes be inaccurate. In addition, the period of these deviations is longer than the window period of the used recursive median filters. Therefore, the recursive median filters cannot remove these deviations. In our future research, some approaches will be proposed to eliminate the singular points of the iterative position and attitude estimation algorithms, which are out of the scope of this report.

6.   Conclusion

This report proposes robust low-cost and real-time position and attitude estimation algorithms based on ground-based beacons and magnetometers. Three sets of ULAs equipped on the object with distinguishable work frequencies receive signals transmitted from three ground-based beacons. The directions of the AOA vectors are estimated by fast 2-D DOA estimation algorithm. Based on the prior knowledge of initial attitude parameters, the position of the object is estimated based on a 3-D AOA location algorithm. Based on the position estimation results, current attitude parameters are updated and used to estimate the position parameters in the next estimation cycle. A recursive median filter is applied to remove large deviations from the estimation results and improve the performance. Simulations show that the proposed low-cost and real-time algorithms successfully estimate the position and attitude most of the time. The algorithms developed for this technique are applicable to the special case of a perfectly vertical magnetic field, thus additional angular transforms would need to be introduced for solutions to more general magnetic orientation cases.

7. References

1. Lee, T.; Sanyal, A.; Leok, M.; McClamroch, N. H. Deterministic Global Attitude Estimation. *Proceedings of the 45th IEEE Conference of Decision and Control*, San Diego, CA, December 2006; pp 3174–3179.

2. Siouris, G. *Missile Guidance and Control*; Springer: New York, 2004.

3. Etkins, B. *Dynamics of Atmospheric Fight*; Dover Publications: Mineola, NY, 1972.

4. Rappaport, T. S.; Reed, J. H.; Woerner, B. D. Position Location Using Wireless Communications on Highways of the Future. *IEEE Comm. Magazine* **1996**, *34* (10), 33–41.

5. Fang, B. T. Simple Solutions for Hyperbolic and Related Position Fixes. *IEEE Trans. Aerospace Elect. Sys.* **1990**, *26* (5), 748–753.

6. Smith, O. J.; Abel, J. S. The Spherical Interpolation Method of Source Localization. *IEEE J. Oceanic Eng.* **1987**, *OE-12* (1), 246–252.

7. McGillem, C. D.; Rappaport, T. S. A Beacon Navigation Method for Autonomous Vehicles. *IEEE Trans. Vehic. Tech.* **1989**, *38* (3), 132–139.

8. Raner, W. H.; Schmidt, M. O. *Fundamentals of Surveying*; Van Nostrand: New York, 1969.

9. Schell, S. V.; Gardner, W. A. *Handbook of Statistics*; Elsevier: New York, 1993; Vol. 10, pp 755–817.

10. Haykin, S., Ed. *Array Signal Processing*; Prentice-Hall: Englewood Cliffs, NJ, 1985.

11. Krim, H.; Viberg, M. Two Decades of Array Signal Processing Reserch: The Parametric Approach. *IEEE Signal Process. Magazine* **1996**, *13*, 67–94.

12. Schmidt, R. Multiple Emitter Location and Signal Parameter Estimation. *IEEE Trans. Antennas Propagation* **1986**, *34* (3), 276–280.

13. Bienvenu, G.; Kopp, L. Principle de la Gonionmetrie Passive Adaptive. *Proceedings 7'eme Colloque GRESIT*, Nice, France, 1979; pp 106/1–106/10.

14. Roy, R.; Paulraj, A.; Kailath, T. Estimation of Signal Parameters via Rotational Invariance Techniques-Esprit. *Proceedings IEEE ICASSP*, Tokyo, Japan, 1986; Vol. 4, pp 2495–2498.

15. Roy, R.; Kailath, T. Esprit-Estimation of Signal Parameters via Rotational Invariance Techniques. *Opt. Eng.* **1990**, *29* (4), 296–313.

16. Wu, Y.; Liao, G.; So, H. C. A Fast Algorithm for 2-D Direction-of-Arrival Estimation. *Signal Processing* **2003**, *83* (8), 1827–1831.

17. Tayem, N.; Kwon, H. M. Azimuth and Elevation Angle Estimation With No Failure and No Eigen Decomposition. *Signal Processing* **2006**, *86* (1), 8–16.

18. Egziabher, D. G.; Elkaim, G. H. Mav Attitude Determination by Vector Matching. *IEEE Trans. Aerospace Elect. Sys.* **2008**, *44* (3), 1012–1028.

19. Lerner, G. M. *Spacecraft Attitude Determination and Control*; D. Reidel Publishing Co.: Dordrecht, The Netherlands, 1978; Ch. 3, pp 420–428.

20. Wahba, G. A Least Squares Estimate of Spacecraft Attitude. *SIAM Review* **1965**, *7* (3), 409.

21. Black, H. D. A Passive System for Determining the Attitude of a Satellite. *AIAA Journal* **1964**, *2* (7), 1350–1351.

22. Carta, D. G.; Lackowski, D. H. Estimation of Orthogonal Transformations in Strapdown Inertial Systems. *IEEE Transactions on Automatic Control* **1972**, *AC-17*, 97–100.

23. Bar-Itzhack, I. Y.; Reiner, J. Recursive Attitude Determination From Vector Observations: Direction Cosine Matrix Identification. *Journal of Guidance, Control and Dynamics* **1984**, *7* (1), 51–56.

24. Ickes, B. P. A New Method for Performing Digital Control System Attitude Computations Using Quaternions. *AIAA Journal* **1970**, *8* (1), 13–17.

25. Shuster, M. D.; Oh, S. D. Three-Axis Attitude Determination From Vector Observations. *Journal of Guidance and Control* **1981**, *4* (1), 70–77.

26. Bar-Itzhack, I. Y.; Oshman, Y. Attitude Determination From Vector Observation: Quaternion Estimation. *IEEE Trans. Aerospace Elect. Sys.* **1985**, *AES-21* (1), 128–136.

27. Choukroun, D.; Bar-Itzhack, I. Y.; Oshman, Y. Novel Quaternion Kalman Flter. *IEEE Trans. Aerospace and Elect. Sys.* **2006**, *42* (1), 174–190.

28. Bar-Itzhack, I. Y.; Idan, M. Recursive Attitude Determination From Vector Observation. *J. Guidance, Control, and Dynamics* **1987,** *10* (2), 152–157.

29. Wilson, M. *Attitude Determination With Magnetometers for Gun-Launched Munitions*; ARL-TR-3209; U.S. Army Research Laboratory: Aberdeen Proving Ground, MD, August 2004.

30. Wilson, M. J. *Nonlinear Projectile Attitude Estimation With Magnetometers and Angular Rate Sensors*; Master's Thesis, University of Delaware, Newark, DE, August 2006.

31. Wilson, M. J. *Projectile Navigation and the Application to Magnetometers,* 1st ed.; Ph.D. Thesis, University of Delaware, Newark, DE, August 2007.

32. Arce, G. R. *Nonlinear Signal Processing*; John Wiley and Sons, Inc.: Hoboken, NJ, 2005.

Appendix. Fast Two-Dimensional Direction of Arrival Estimation Algorithm

Consider one impinging signal represented by the vector $\vec{s}$ that is received by a set of parallel uniform linear arrays (ULAs) equipped on the object, as shown in figure A-1, and assume that the position of the object is known.

Figure A-1. One impinging signal is received by the system of three parallel ULAs equipped on the object.

When the fast two-dimensional direction of arrival estimation algorithm is used, the elevation angle α and the azimuth angle β are estimated as $\hat{\alpha}$ and $\hat{\beta}$, respectively. According to the cosine theorem, the included angle between the X_b axis and $\vec{s}$ is

$$\omega_x = \cos^{-1}(\cos\beta\cos(90° - \alpha)) = \cos^{-1}(\cos\beta\sin\alpha). \tag{A-1}$$

The direction of $\vec{s}$ in the Earth-fixed coordinate can be determined by the positions of the beacon and the object. Based on the signal direction $\vec{s}$ and the included angle ω, a cone with an axis of $\vec{s}$ can be determined, on whose surface infinite, body-fixed coordinates can be found to satisfy the estimated elevation and azimuth angles. Figure A-2 shows two sets of body-fixed coordinates (X_b, Y_b, Z_b) and (X_b', Y_b', Z_b') satisfying the given conditions. Therefore, given the position of the object, one angle of arrival (AOA) vector is not sufficient to determine the attitude of the object.
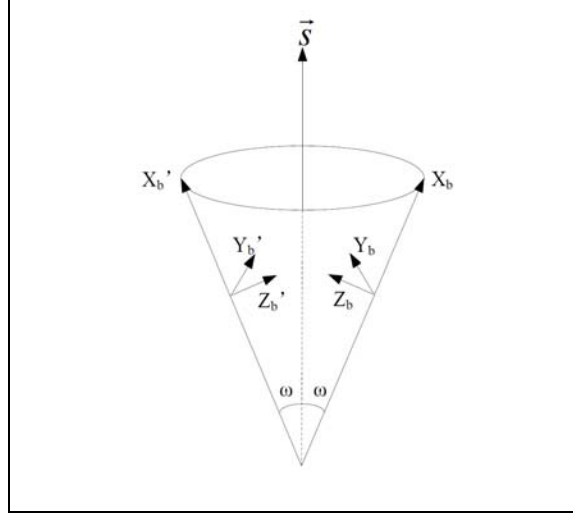
Figure A-2. One impinging signal determines a cone, on whose surface infinite body-fixed coordinates can be found to satisfy the estimated elevation and azimuth angles.

If two impinging signals are transmitted with direction vectors of $\vec{s}_1$ and $\vec{s}_2$, two cones with axes of $\vec{s}_1$ and $\vec{s}_2$ are determined by the included angle between the X_b axis and the vector directions. Let the centers of the undersurfaces of the two cones be O_1 and O_2. There are at most two intersection lines between the two cones, $\overline{OA}$ and $\overline{OB}$, as shown in figure A-3. Let the estimated elevation and azimuth angles from the first impinging signal be ($\hat{\alpha}_1, \hat{\beta}_1$) and the estimated elevation and azimuth angles from the second impinging signal be ($\hat{\alpha}_2, \hat{\beta}_2$). In figure A-3, assume that the body-fixed coordinate (X_b, Y_b, Z_b) on the intersection line $\overline{OA}$ satisfies the elevation and azimuth angles ($\hat{\alpha}_1$, $\hat{\beta}_1$) and ($\hat{\alpha}_2$, $\hat{\beta}_2$) with respect to $\vec{s}_1$ and $\vec{s}_2$, respectively. On the intersection line $\overline{OB}$, body-fixed coordinate (X_b', Y_b', Z_b') satisfies the elevation and azimuth angles ($\hat{\alpha}_1$, $\hat{\beta}_1$) with respect to $\vec{s}_1$. Body-fixed coordinate (X_b'', Y_b'', Z_b'') satisfies the elevation and azimuth angles ($\hat{\alpha}_2$, $\hat{\beta}_2$) with respect to $\vec{s}_2$, where X_b' overlaps X_b''. Thus, only (X_b, Y_b, Z_b) satisfies all of the given conditions. In conclusion, given the position of the object, two linearly independent AOA vectors are sufficient to determine the attitude of the object.
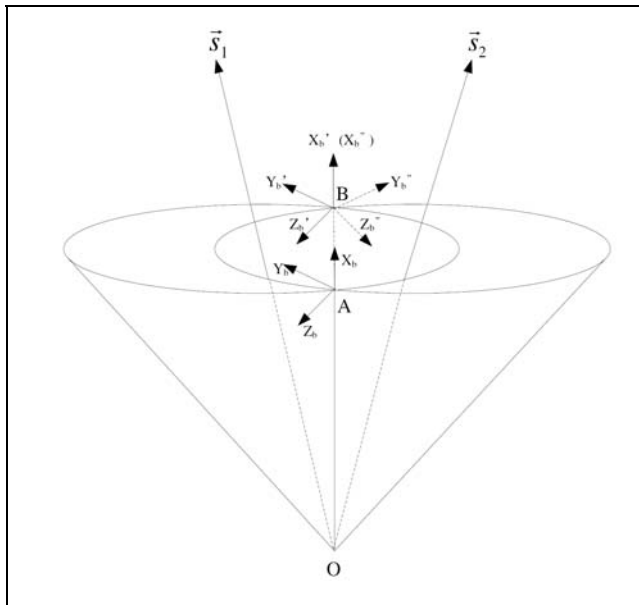
Figure A-3. Two impinging signals determine a pair of
attitudes of the object.

NO. OF
COPIES ORGANIZATION

1   DEFENSE TECHNICAL
(PDF   INFORMATION CTR
only)   DTIC OCA
        8725 JOHN J KINGMAN RD
        STE 0944
        FORT BELVOIR VA 22060-6218

1   DIRECTOR
        US ARMY RESEARCH LAB
        IMNE ALC HRR
        2800 POWDER MILL RD
        ADELPHI MD 20783-1197

1   DIRECTOR
        US ARMY RESEARCH LAB
        RDRL CIM L
        2800 POWDER MILL RD
        ADELPHI MD 20783-1197

1   DIRECTOR
        US ARMY RESEARCH LAB
        RDRL CIM P
        2800 POWDER MILL RD
        ADELPHI MD 20783-1197

1   DIRECTOR
        US ARMY RESEARCH LAB
        RDRL D
        2800 POWDER MILL RD
        ADELPHI MD 20783-1197

        ABERDEEN PROVING GROUND

1   DIR USARL
        RDRL CIM G (BLDG 4600)

INTENTIONALLY LEFT BLANK.